Prediction of Bandlimited Fading Envelopes with Arbitrary Spectral Shape

Raphael J. Lyman and Adam Sikora

Abstract

In mobile radio, fading-envelope prediction can improve the performance of adaptive modulation techniques that require up-to-date channel-state information for optimal performance. We show how to compute the minimum mean squared prediction error of a mobile-radio fading envelope modeled as a stationary, bandlimited process arising from a diffuse set of local scatterers. For bandlimited processes, it is difficult to solve for the Wiener predictor using the usual spectral-factorization approach. Our method reduces the prediction problem to an eigenvalue decomposition, and is appropriate when the prediction is to be based on error-corrupted estimates of a narrowband fading process. We also show how to bound the error in the computation due to truncation of infinite series.

Index Terms

Fading, prediction, bandlimited.

I. Introduction

In mobile radio, adaptive modulation requires the use of fading-envelope prediction to overcome delays in feeding channel-state information back from receiver to transmitter [1], [2]. In this paper, we show how to compute the minimum mean squared prediction error of a fading envelope modeled as a stationary, bandlimited process arising from a diffuse set of local scatterers. The prediction is based on estimates of the fading envelope over a finite interval of past values, with the estimation errors on this interval modeled as white noise.

Our approach reduces the prediction problem to an eigenvalue decomposition [3, p. 242]. This has advantages over the more-common spectral-factorization approach [3, Sec. 11-6] when the

The authors are on the faculty of New Mexico State University, Las Cruces. R. J. Lyman is with the Klipsch School of Electrical and Computer Engineering, and A. Sikora is with the Department of Mathematical Sciences.

prediction is to be based on error-corrupted estimates of a narrowband fading process, because the spectrum of such a process exhibits a discontinuity, or a very steep transition, at the maximum Doppler frequency, and is thus difficult to approximate with a rational function. The eigenvalue problem can be formulated in either the time or frequency domain, providing a convenient solution method when either the autocorrelation or power spectral density of the fading process is specified. We also provide a method for bounding the error in the computation due to truncation of infinite series.

This paper provides a solution method for bandlimited fading envelopes with arbitrary spectral shape. It thus generalizes the methods we have developed for important special cases [4], [5]. Example curves are shown for a fading envelope having a Aulin-type Doppler spectrum [6]. We note that preliminary findings of this research were previously presented at ICASSP [7].

II. Prediction of the Fading Envelope

Let $u(t)$ be the complex baseband representation of a carrier-based transmitted signal. Then the effect of a flat-fading channel may be modeled by (see, e.g., Stuber [8, p. 216])

$$r(t) = c(t)u(t) + v(t), \tag{1}$$

where $c(t) = x(t) + jy(t)$ is the *complex fading envelope* and $v(t)$ is additive noise. If the fading results from a large number of independent scatterers, which are distributed evenly in every direction with respects to the receiver, $x(t)$ and $y(t)$ may be modeled as zero-mean, independent, stationary Gaussian processes with identical autocorrelation functions [8, p. 39]. For this reason, let us consider just one component, $x(t)$, of the fading envelope. Suppose we wish to predict a future value, $x(r)$, based on an estimate of past values

$$\tilde{x}(t) = x(t) + e(t) \quad t \in [r - \tau - T, r - \tau], \tag{2}$$

where τ and T are positive, and $e(t)$ represents the estimation errors. These errors are modeled as zero-mean white noise with power spectral density σ_e^2, and are uncorrelated with $x(t)$. A linear predictor takes the form

$$\hat{x}(r) = \int_{r-\tau-T}^{r-\tau} \tilde{x}(t)h(r-t)dt. \tag{3}$$

We seek a function $h(t)$ that minimizes the mean squared prediction error,

$$J = \mathcal{E}\{[x(r) - \hat{x}(r)]^2\}. \tag{4}$$

This model assumes that the value of $\tilde{x}(t)$ is known over the entire continuum of a T-length interval. In digital radio, though, channel conditions are often tracked using adaptive algorithms that yield estimates of the fading envelope at discrete times, updating once each time a new symbol is received (see, e.g., Proakis [9, Sec. 11.1.7]). These estimates may be interpreted as a sampled waveform. Since the waveform is sampled only over a finite interval, some signal information is lost in the discretization process. Thus, the predictability of $x(t)$ may be affected by the choice of sample rate. If, on the other hand, the channel variations are much slower than the transmission rate, as is usually the case in practice, then the fading envelope will remain nearly constant over a symbol duration, and little information will be lost. Thus, a prediction based on discrete estimates of the fading envelope can be expected to approach the performance of a continuous-time predictor.

Furthermore, an optimal continuous-time predictor will not be outperformed by any discrete-time predictor, since it makes use of all the information on the T-length interval of past values. Thus, a predictability analysis based on a continuous-time model provides a useful performance bound over the entire class of linear predictors.

Now, because of the stationarity of $\tilde{x}(t)$, J does not depend on r. This may be verified easily by substituting (2) and (3) into (4) and expanding. Note that the lack of an r dependency results from the fact that the prediction is based on a sliding T-length window of estimates (2) that is always τ seconds in the past with respects to r. Thus, making use of (2), (3) and (4), and letting $r = \tau + \frac{T}{2}$ we have

$$\begin{aligned} J &= \mathcal{E}\left\{\left[x(\tau+\tfrac{T}{2}) - \int_{-\frac{T}{2}}^{\frac{T}{2}} \tilde{x}(t)h(\tau+\tfrac{T}{2}-t)dt\right]^2\right\} \\ &= \mathcal{E}\left\{\left[x(\tau+\tfrac{T}{2}) - \int_{-\frac{T}{2}}^{\frac{T}{2}} x(t)h(\tau+\tfrac{T}{2}-t)dt \right.\right. \\ &\qquad \left.\left. - \int_{-\frac{T}{2}}^{\frac{T}{2}} e(t)h(\tau+\tfrac{T}{2}-t)dt\right]^2\right\} \end{aligned}$$

$$= \mathcal{E}\left\{\left[x(\tau+\tfrac{T}{2}) - \int_{-\frac{T}{2}}^{\frac{T}{2}} x(t)h(\tau+\tfrac{T}{2}-t)dt\right]^2\right\}$$
$$+ \mathcal{E}\left\{\left[\int_{-\frac{T}{2}}^{\frac{T}{2}} e(t)h(\tau+\tfrac{T}{2}-t)dt\right]^2\right\}, \quad (5)$$

because $x(t)$ and $e(t)$ are uncorrelated. Note that we have chosen r such that the limits of integration in (5) are symmetric. This is advantageous since it leads to a symmetric eigenvalue problem in what follows.

To find the optimal predictor, we first express $h(t)$ as an expansion [3, App. 2],

$$h(t) = \sum_{n=0}^{\infty} a_n \phi_n(\tau+\tfrac{T}{2}-t) \quad t \in [\tau, \tau+T], \quad (6)$$

with $\{\phi_n(t)\}$ the countable orthogonal solutions of

$$\int_{-\frac{T}{2}}^{\frac{T}{2}} \phi(s) R_{xx}(t-s)ds = \lambda\phi(t), \quad (7)$$

where $R_{xx}(t)$ is the autocorrelation of $x(t)$ and $\lambda \neq 0$. Since $R_{xx}(t)$ is real valued, has even symmetry, and is nonnegative definite, the eigenvalues $\{\lambda_n\}$ are real and positive, and the eigenfunctions $\{\phi_n(t)\}$ may be taken as real. We order the eigenvalues such that $\lambda_{n+1} \leq \lambda_n$, and in keeping with the convention of Slepian, et al. [10], we scale each $\phi_n(t)$ such that

$$\int_{-\frac{T}{2}}^{\frac{T}{2}} \phi_n^2(t)dt = \lambda_n. \quad (8)$$

The expansion (6) is valid if $\{\phi_n(t)\}$ is complete on $t \in [-\frac{T}{2}, \frac{T}{2}]$. This is assured if $R_{xx}(t)$ is positive definite [3, p. 374]; that is, if

$$\int_{-\frac{T}{2}}^{\frac{T}{2}} \int_{-\frac{T}{2}}^{\frac{T}{2}} R_{xx}(t-s) f(s) f^*(t)\, ds\, dt > 0 \quad (9)$$

for any $f(t)$ with

$$\int_{-\frac{T}{2}}^{\frac{T}{2}} |f(t)|^2 dt > 0. \quad (10)$$

To determine a sufficient condition to satisfy (9), let $f(t) = 0$ for $t \notin [-\frac{T}{2}, \frac{T}{2}]$. Then, writing $R_{xx}(t)$ as the inverse Fourier transform of the power spectral density, $S_{xx}(\omega)$, and changing the order of integration, it is not difficult to show that

$$\int_{-\frac{T}{2}}^{\frac{T}{2}} \int_{-\frac{T}{2}}^{\frac{T}{2}} R_{xx}(t-s) f(s) f^*(t)\, ds\, dt$$
$$= \frac{1}{2\pi} \int_{-\infty}^{\infty} S_{xx}(\omega) |F(\omega)|^2 d\omega, \quad (11)$$

where $F(\omega)$ is the Fourier transform of $f(t)$. Now $f(t)$ is time limited and, from (10), not identically zero. Thus we can have $F(\omega) = 0$ only on a set of zero measure. Hence, if $S_{xx}(\omega) > 0$ on a set of positive measure, (11) shows that (9) is satisfied.

This condition on $S_{xx}(\omega)$ is met whenever the fading envelope is modeled as arising from a diffuse set of local scatterers, as it often is when the number of scatterers is considered to be large, and thus not individually resolvable (see e.g. Clarke [11]). Such might be the case in a dense urban environment, for example. If only a small number of scatterers are present, then $S_{xx}(\omega)$ is often modeled as a line spectrum. In this case, the fading envelope may be predicted by estimating the sinusoidal fading parameters of each received signal path, and then extrapolating the sum of sinusoids into the future (see, e.g., Andersen et al. [12]).

Now, bearing in mind our restriction on the support of $S_{xx}(\omega)$, it may be shown that (see appendix)

$$\begin{aligned} &\mathcal{E}\left\{\left[x(\tau+\tfrac{T}{2}) - \int_{-\frac{T}{2}}^{\frac{T}{2}} x(t)h(\tau+\tfrac{T}{2}-t)dt\right]^2\right\} \\ &= \quad R_{xx}(0) - 2\sum_{n=0}^{\infty} a_n\lambda_n\phi_n(\tau+\tfrac{T}{2}) + a_n^2\lambda_n^2, \end{aligned} \tag{12}$$

where each $\phi_n(t)$ is defined for all t by (7).

Considering now the error term of (5) we have, by a similar process,

$$\begin{aligned} &\mathcal{E}\left\{\left[\int_{-\frac{T}{2}}^{\frac{T}{2}} e(t)h(\tau+\tfrac{T}{2}-t)dt\right]^2\right\} \\ &= \quad \sigma_e^2\sum_{n=0}^{\infty} a_n^2\lambda_n. \end{aligned} \tag{13}$$

Thus, combining (5), (12), and (13) we have

$$J = R_{xx}(0) + \sum_{n=0}^{\infty} -2a_n\lambda_n\phi_n(\tau+\tfrac{T}{2}) + a_n^2\lambda_n(\lambda_n+\sigma_e^2). \tag{14}$$

Setting the partial derivatives to zero we have

$$\frac{\partial J}{\partial a_k} = -2\lambda_k\phi_k(\tau+\tfrac{T}{2}) + 2a_k\lambda_k(\lambda_k+\sigma_e^2) = 0. \tag{15}$$

Solving for a_k yields

$$a_k = \frac{\phi_k(\tau+\frac{T}{2})}{\lambda_k+\sigma_e^2}. \tag{16}$$

This may be substituted into (6) to obtain $h(t)$. Thus, the predictor (3) is determined.

Note that the expression (16) for the coefficients $\{a_k\}$ has the same form as the expression we previously found for bandlimited processes with flat spectral densities [4, eq. 14]. In that case, σ_e^2 was interpreted as a Lagrange multiplier arising from an energy constraint. The basis functions $\{\phi_n(t)\}$ were the prolate spheroidal wave functions [10], which are the solutions of (7) when

$$R_{xx}(t) = \frac{\sin \Omega t}{\pi t}, \tag{17}$$

with $\Omega > 0$ the band limit of the fading process $x(t)$. The solution presented in this paper generalizes those results, by accommodating processes with a wider class of spectral densities, including non-bandlimited processes. On the other hand, since mobile-radio fading envelopes are often modeled as bandlimited [6], [11], [13], it is important to note that for such processes, the modeling of estimation errors $e(t)$ in (5) is critical, since the optimization problem otherwise fails to have a solution [14].

When estimation errors are modeled, the predictor problem can be solved by factoring the spectrum [3, Sec. 11.6], as is often done in Wiener problems. But for bandlimited and narrowband fading envelopes, this approach is difficult, because the spectrum of the error-corrupted estimates is discontinuous, or exhibits a steep transition, at the maximum Doppler frequency $f_m = \Omega/2\pi$. Such a spectrum can be difficult to approximate using a rational function. Our approach also affords a convenient separation of the statistics for the fading envelope from those of the estimation errors. Note that the eigenvalue problem (7) does not depend on the statistics of the error $e(t)$; the effect of estimation errors on the optimal predictor may be studied simply by varying σ_e^2 in (16), the coefficients of the predictor impulse response.

III. Bandlimitedness and the Mean Squared Error

We may also substitute (16) into (14) to get the minimum mean square prediction error,

$$J_{\min} = R_{xx}(0) - \sum_{n=0}^{\infty} \lambda_n \frac{\phi_n^2(\tau + \frac{T}{2})}{\lambda_n + \sigma_e^2}. \tag{18}$$

To simplify this expression, we would like to expand $R_{xx}(t)$ in terms of $\{\phi_n(\tau + \frac{T}{2})\}$. To do this, we might think of substituting $s = 0$ in Mercer's theorem,

$$R_{xx}(t-s) = \sum_{n=0}^{\infty} \phi_n(s)\phi_n(t) \quad |s|, |t| \le \tfrac{T}{2}, \tag{19}$$

but this would allow for expansion in $\{\phi_n(t)\}$ only for $|t| \leq \frac{T}{2}$. As noted before, though, the mobile radio fading envelope is usually modeled as bandlimited, and in this case, the expansion is valid for all t. To see this, define

$$\phi^D(t) = \phi(t)\Pi\left(\tfrac{t}{T}\right) \tag{20}$$

where

$$\Pi(t) = \begin{cases} 1 & |t| \leq \frac{1}{2} \\ 0 & \text{otherwise.} \end{cases} \tag{21}$$

The Fourier transform of (20) is

$$\Phi^D(\omega) = \int_{-\infty}^{\infty} \Phi(\eta) \frac{\sin \frac{T}{2}(\omega - \eta)}{\pi(\omega - \eta)}\, d\eta. \tag{22}$$

Also, the Fourier transform of (7) is

$$\Phi^D(\omega) S_{xx}(\omega) = \lambda \Phi(\omega). \tag{23}$$

Now suppose

$$S_{xx}(\omega) = 0 \quad |\omega| > \Omega. \tag{24}$$

Then we may substitute (23) into (22) to obtain

$$\int_{-\Omega}^{\Omega} S_{xx}(\eta)\Phi^D(\eta) \frac{\sin \frac{T}{2}(\omega - \eta)}{\pi(\omega - \eta)}\, d\eta = \lambda \Phi^D(\omega). \tag{25}$$

The countable orthogonal solutions $\{\Phi_n^D(\omega)\}$ of (25) are complete, with respects to $S_{xx}(\omega)$, on the compact interval $\omega \in [-\Omega, \Omega]$, and map one-to-one with $\{\phi_n^D(t)\}$, with the same eigenvalues. The norms of the eigenfunctions may be shown to be (see appendix),

$$\int_{-\Omega}^{\Omega} S_{xx}(\omega) \left|\Phi_n^D(\omega)\right|^2 d\omega = 2\pi\lambda_n^2. \tag{26}$$

Because of the completeness of $\{\Phi_n^D(\omega)\}$, we may expand, for any s,

$$e^{-j\omega s} = \sum_{n=0}^{\infty} b_n \Phi_n^D(\omega), \quad |\omega| \leq \Omega. \tag{27}$$

where, using (26),

$$b_n = \frac{1}{2\pi\lambda_n^2} \int_{-\Omega}^{\Omega} S_{xx}(\omega) e^{-j\omega s} [\Phi_n^D(\omega)]^* d\omega \tag{28}$$

To compute the coefficients, we may use (23),

$$\begin{aligned} b_n &= \frac{1}{2\pi\lambda_n}\int_{-\infty}^{\infty}[\Phi_n(\omega)]^* e^{-j\omega s}d\omega \\ &= \frac{\phi_n(s)}{\lambda_n}. \end{aligned} \tag{29}$$

Thus, combining (27) and (29), and using (23) again,

$$\begin{aligned} e^{-j\omega s} &= \sum_{n=0}^{\infty}\frac{\phi_n(s)}{\lambda_n}\Phi_n^D(\omega), \quad |\omega| \le \Omega \\ e^{-j\omega s}S_{xx}(\omega) &= \sum_{n=0}^{\infty}\phi_n(s)\Phi_n(\omega) \quad \forall \quad s,\omega \\ R_{xx}(t-s) &= \sum_{n=0}^{\infty}\phi_n(s)\phi_n(t) \quad \forall \quad s,t. \end{aligned} \tag{30}$$

Now letting $s = t = \tau + \frac{T}{2}$ in (30) and substituting into (18), we obtain

$$J_{\min} = \sum_{n=0}^{\infty}\phi_n^2(\tau+\tfrac{T}{2})\frac{\sigma_e^2}{\lambda_n+\sigma_e^2}. \tag{31}$$

This expression shows that the mean squared prediction error $J_{\min}$ tends to zero as the estimation error σ_e^2 for past values of the fading envelope $x(t)$ approaches zero. In other words, if the past values of $x(t)$ are known perfectly over any interval of nonzero length, the fading envelope may be predicted arbitrarily far in the future without error. This is an expected result for bandlimited processes, based on our previous findings [14]. Thus, the issue of estimation error dominates the predictability of a bandlimited fading envelope. This key point is made clear by a continuous-time analysis.

Other investigators have shown that discrete-time predictors of bandlimited processes can also achieve arbitrarily small estimation error, but this requires error-free knowledge of the infinite past (see, e.g., Papoulis [15] and references in Lyman et al. [14]). These authors also have not emphasized the effect of estimation errors on the quality of the prediction, nor the application of bandlimited modeling to mobile-radio fading.

Now, when computing values for $J_{\min}$, we truncate the infinite series in (31). To bound the error introduced by this truncation we define

$$\underline{J}_{\min} = \sum_{n=0}^{N-1}\phi_n^2(\tau+\tfrac{T}{2})\frac{\sigma_e^2}{\lambda_n+\sigma_e^2}. \tag{32}$$

Clearly, $\underline{J}_{\min} \leq J_{\min}$. Further, it may be shown (see appendix) that by defining

$$\overline{J}_{\min} = R_{xx}(0) - \sum_{n=0}^{N-1} \phi_n^2(\tau + \tfrac{T}{2}) \frac{\lambda_n}{\lambda_n + \sigma_e^2}, \tag{33}$$

we have

$$\underline{J}_{\min} \leq J_{\min} \leq \overline{J}_{\min}. \tag{34}$$

Note that these bounds may not be valid if the fading envelope $x(t)$ is not bandlimited.

IV. Computational Issues and Results

To compute $J_{\min}$, we may solve (7) numerically and substitute the values into (31) [7]. This requires knowledge of $R_{xx}(t)$. Some bandlimited fading models, though, are more easily characterized in the frequency domain, with simple expressions for $S_{xx}(\omega)$, but with autocorrelation functions that are difficult–or impossible–to obtain in closed form [6], [13]. Values for $R_{xx}(t)$ may be obtained by numerically evaluating the inverse Fourier transform of $S_{xx}(\omega)$, but this is not simply a matter of taking an IDFT, because of our interest in the finite intervals $\omega \in [-\Omega, \Omega]$ and $t \in [-\frac{T}{2}, \frac{T}{2}]$.

Computing values for $R_{xx}(t)$ can be avoided by solving numerically for the basis functions $\Phi_n^D(\omega)$ directly in the frequency domain using (25), which is equivalent to the time-domain equation (7). Using the Nystrom method [16, p. 791], [7], we approximate the integral in (25) with an M-point quadrature rule, then evaluate the equation at the quadrature points. The resulting discretized eigenvalue problem may be placed in matrix form by defining an $M \times M$ matrix K with

$$[K]_{i,j} = S_{xx}(\eta_j) w_j \frac{\sin \frac{T}{2}(\eta_i - \eta_j)}{\pi(\eta_i - \eta_j)}, \tag{35}$$

where $\{w_j\}$ are the weights of the quadrature rule and $\{\eta_j\}$ are the quadrature points, extending along the interval $\eta \in [-\Omega, \Omega]$.

An eigenvalue decomposition of K yields a matrix whose columns are approximate basis functions, $\{\Phi_n^D(\eta_j)\}_{n=0}^{M-1}$ evaluated at $\{\eta_j\}_{j=1}^{M}$, as well as eigenvalues $\{\lambda_n\}_{n=0}^{M-1}$. The required values $\{\phi_n(\tau + \frac{T}{2})\}$ for substitution in (31) can be obtained by making use of (23) to numerically compute the inverse Fourier transform of $\{\Phi_n(\omega)\}$,

$$\phi_n(t) = \frac{1}{2\pi\lambda_n} \int_{-\Omega}^{\Omega} S_{xx}(\omega) \Phi_n^D(\omega) e^{j\omega t} d\omega. \tag{36}$$

Note that the same quadrature rule can be used as was applied in (35), making it unnecessary to interpolate values for $\Phi_n^D(\omega)$. This step is analogous to the extrapolation of $\{\phi_n(t)\}$ when the problem is worked in the time domain [7, Eq. 23]. Thus, eliminating the inverse Fourier transform at the beginning of the process results in genuine simplification.

Care should be exercised in choosing a quadrature rule. Because bandlimited processes have smooth autocorrelation functions, Gaussian quadrature can be used when working the eigenvalue problem in the time domain [16, Sec. 4.5], [7]. On the other hand, the power spectral density may be discontinuous, or have discontinuous derivatives (see, e.g., Aulin [6]). In this case, a more straightforward form of quadrature, such as the trapezoidal rule [16, p. 133], may be appropriate.

Also, in (35), note that though the sinc kernel is symmetric, the matrix K is not. Symmetry can be restored to the eigenvalue problem, though, using a straightforward technique [16, p. 794].

The frequency-domain approach that we have just described was used to compute the sets of basis functions $\phi_n(t)$ shown in Figure 1. For these graphs, we let $\Omega = 1$ and $T = 2$, and we used a 101-point trapezoidal rule for quadrature. The first graph shows the first six basis functions appropriate for a bandlimited fading envelope with $S_{xx}(\omega) = 1$ for $|\omega| \leq \Omega$. As was discussed previously, these basis functions are the prolate spheroidal wave functions, whose properties are described more fully by Slepian et al. [10], Frieden [17] and Papoulis [18, p. 205]. Note that for this graph, using Slepian's notation, we have $c = \frac{\Omega T}{2} = 1$.

The second graph of Figure 1 shows the basis functions appropriate for the popular fading model developed by R. H. Clarke [11], [19, Ch. 1]. Using Clarke's approach, and assuming that the local scatterers are distributed evenly in every direction with respects to the receiver, the power spectral density may be written as

$$S_{xx}(\omega) = \begin{cases} \dfrac{2}{\pi\sqrt{1 - \frac{\omega^2}{\Omega^2}}} & |\omega| < \Omega \\ 0 & \text{otherwise.} \end{cases} \tag{37}$$

The scaling in (37) was chosen so that the fading process powers $R_{xx}(0) = \frac{\Omega}{\pi}$ represented by the two graphs in Figure 1 would be the same. Identical graphs were obtained when the basis functions were computed using the time-domain approach, in which (7) was solved instead of (25), using a 96-point Gaussian quadrature rule [20, p. 919]. In these computations, (17) was used for the flat spectral density case, and $R_{xx}(t) = \frac{\Omega}{\pi} J_0(\Omega t)$ was used for the Clarke model.

In our previous work, we developed methods for computing the predictability of bandlimited fading envelopes with flat and Clarke-type spectra [4], [5]. Those approaches required the use of special functions that exhibited appropriate orthogonality properties with respects to the spectrum of interest. The approach developed in this paper, though, may be applied even if no such special functions are known.

Consider, for example, the Aulin fading model [6], [13]. It is a modification of the Clarke model intended to account for scattered signal components arriving at the receiver from angles of elevation other than horizontal. If the angles of arrival are distributed as

$$p_\beta(\beta) = \begin{cases} \dfrac{\cos\beta}{2\sin\beta_{\max}}, & |\beta| \le \beta_{\max} \le \dfrac{\pi}{2} \\ 0 & \text{otherwise,} \end{cases} \tag{38}$$

then the power spectral density of the fading envelope may be written most succinctly as in Qu and Yeap [13, Eq. 15]. Neither Aulin nor Qu and Yeap offer an expression for $R_{xx}(t)$ in closed form.

Plots of Aulin spectra are shown in Figure 2 for several values of $\beta_{\max}$. These plots are scaled, again, such that $R_{xx}(0) = \frac{\Omega}{\pi}$. Note that if $\beta_{\max} > 0$, the spectrum includes a constant-value segment near $\pm\Omega$. For $\beta_{\max} = 0$, the Aulin model is the same as the Clarke model (37), and the spectrum approaches $+\infty$ as $|\omega| \to \Omega$. If $\beta_{\max} = \frac{\pi}{2}$, then the spectrum is flat within the band limits.

Using a trapezoidal rule for quadrature in (35), with $M = 101$, and using the same rule for obtaining $\{\phi_n(\tau + \frac{T}{2})\}$ by inverse transform, as discussed above, the curves of Figures 3–6 were computed from (31). The series in (31) was truncated to $N = 24$ terms, which can be shown to result in negligible error, using the techniques from Section III. The curves in Figure 3 show the minimum mean squared prediction error of an Aulin-type mobile-radio fading envelope with $\beta_{\max} = 30°$, and with $\Omega = 10, 20, \ldots, 50$. The prediction is based on past estimates over an interval of length $T = 0.2$ sec., and predicts the value of the fading envelope $\tau = .04$ sec. in the future. The prediction error is expressed in decibels with respects to the power of the fading process, $R_{xx}(0)$. The horizontal axis shows the parameter-to-estimation error ratio, $R_{xx}(0)/\sigma_e^2$. Note that, as the estimation error decreases, the prediction error approaches zero. As was mentioned previously, this is a general property of bandlimited processes [14].

The graph in Figure 4 was obtained when T was increased to 0.8 sec. It shows a small

performance gain achieved by lengthening the interval of past estimates upon which the fading-envelope prediction is based. In our computations, increasing T beyond 0.8 sec. did not result in any significant additional improvement. If T is returned to 0.2 sec., and τ is increased to .08 sec., the curves in Figure 5 result. As expected, the predictor performance degrades as we attempt to predict further into the future.

The effect of the fading-envelope model is shown in Figure 6. For these curves, $\Omega = 10$, $T = 0.2$ sec., and $\tau = .04$ sec. Prediction performance is shown for fading envelopes with a Clarke spectrum, an Aulin spectrum with $\beta_{\max} = 30°$, and a flat spectrum. The area of the graph corresponds to the small rectangular box near the center of Figure 3. Note that the performance variation resulting from the choice of fading model is less than 0.4 dB. On the other hand, Figures 3–5 show that even a small variation in Ω causes a large change in prediction error. This suggests that the predictability of the mobile-radio fading envelope may be more profoundly affected by the maximum Doppler frequency than by the exact shape of the Doppler spectrum.

V. Conclusions

The approach described in this paper for computing the predictability of the mobile-radio fading envelope is more flexible and easier to implement than those we have described previously. As we have discussed, previous computations required the choice of special functions with the appropriate orthogonality properties. For fading envelopes with flat bandlimited spectra, we used the prolate spheroidal wave functions [4]. In that case, we employed tabulated values, since quality software for computing these functions was not easy to find. For the Clarke-type fading envelope, Legendre and Chebyshev polynomials were used [5]. These were easier to compute, but the predictability computation required the numerical evaluation of a matrix of integral inner products between these two sets. The new approach avoids all these difficulties, and can be used for any fading envelope with a diffuse spectrum.

As we have noted, in mobile radio, the fading envelope is often modeled as a bandlimited process. In this case, the prediction problem may be worked directly in the frequency domain, with knowledge of the power spectral density, or Doppler spectrum. Bandlimitedness also allows us to bound the error in the predictability computation caused by the truncation of infinite series. We feel that these findings, and those of other investigators, suggest a strong potential for applying the theory of bandlimited processes to the problem of fading compensation (see, e.g., Baddour

and Beaulieu [21]).

Predictability analysis can be useful for adaptive transmission, or any fading compensation technique that uses estimates of current channel conditions. Such approaches will usually degrade if those estimates are in error, or involve significant delays (see, e.g., Goldsmith and Chua [22]). Our work shows how delay and estimation error are related, because a bandlimited process that is known without error on an interval of nonzero length is perfectly predictable [14]. Thus, if the estimation error is sufficiently small, prediction may be used to overcome the delay. For this reason, the issue of channel estimation errors is critically important in determining whether prediction may be used successfully in an adaptive transmission system.

APPENDIX

In this appendix, we derive in detail some of the results presented in the main body of the paper. To show (12), we note that, as we have discussed, if $S_{xx}(\omega) > 0$ on a set of positive measure, then the expansion (6) is valid. Thus,

$$\begin{aligned}
&\mathcal{E}\left\{\left[x(\tau+\tfrac{T}{2}) - \int_{-\frac{T}{2}}^{\frac{T}{2}} x(t)h(\tau+\tfrac{T}{2}-t)dt\right]^2\right\} \\
&= \mathcal{E}\Bigg\{x^2(\tau+\tfrac{T}{2}) \\
&\qquad - 2\int_{-\frac{T}{2}}^{\frac{T}{2}} x(\tau+\tfrac{T}{2})x(t)h(\tau+\tfrac{T}{2}-t)\,dt \\
&\qquad + \int_{-\frac{T}{2}}^{\frac{T}{2}}\int_{-\frac{T}{2}}^{\frac{T}{2}} x(t)x(s)h(\tau+\tfrac{T}{2}-t) \\
&\qquad\qquad \cdot h(\tau+\tfrac{T}{2}-s)\,dt\,ds\Bigg\} \\
&= R_{xx}(0) - 2\int_{-\frac{T}{2}}^{\frac{T}{2}} R_{xx}(\tau+\tfrac{T}{2}-t)h(\tau+\tfrac{T}{2}-t)\,dt \\
&\quad + \int_{-\frac{T}{2}}^{\frac{T}{2}}\int_{-\frac{T}{2}}^{\frac{T}{2}} R_{xx}(t-s)h(\tau+\tfrac{T}{2}-t) \\
&\qquad \cdot h(\tau+\tfrac{T}{2}-s)\,dt\,ds
\end{aligned}$$

$$
\begin{aligned}
&= R_{xx}(0) \\
&\quad - 2\int_{-\frac{T}{2}}^{\frac{T}{2}} R_{xx}(\tau+\tfrac{T}{2}-t)\sum_{n=0}^{\infty} a_n\phi_n(t)\,dt \\
&\quad + \int_{-\frac{T}{2}}^{\frac{T}{2}}\int_{-\frac{T}{2}}^{\frac{T}{2}} R_{xx}(t-s) \\
&\qquad \cdot \sum_{n=0}^{\infty}\sum_{p=0}^{\infty} a_n a_p \phi_n(t)\phi_p(s)\,dt\,ds \\
&= R_{xx}(0) \\
&\quad - 2\sum_{n=0}^{\infty} a_n \int_{-\frac{T}{2}}^{\frac{T}{2}} \phi_n(t) R_{xx}(\tau+\tfrac{T}{2}-t)\,dt \\
&\quad + \sum_{n=0}^{\infty}\sum_{p=0}^{\infty} a_n a_p \int_{-\frac{T}{2}}^{\frac{T}{2}} \phi_n(t) \\
&\qquad \cdot \left[\int_{-\frac{T}{2}}^{\frac{T}{2}} \phi_p(s) R_{xx}(t-s)\,ds\right] dt \\
&= R_{xx}(0) - 2\sum_{n=0}^{\infty} a_n\lambda_n\phi_n(\tau+\tfrac{T}{2}) \\
&\quad + \sum_{n=0}^{\infty}\sum_{p=0}^{\infty} a_n a_p \lambda_p \int_{-\frac{T}{2}}^{\frac{T}{2}} \phi_n(t)\phi_p(t)\,dt \\
&= R_{xx}(0) - 2\sum_{n=0}^{\infty} a_n\lambda_n\phi_n(\tau+\tfrac{T}{2}) + a_n^2\lambda_n^2,
\end{aligned}
\tag{39}
$$

where (6), (8) and the orthogonality of $\{\phi_n(t)\}$ were used, and where each $\phi_n(t)$ is defined for all t by (7).

Now, to determine the norms of the eigenfunctions of (25), we make use of (8), (23) and (24) to obtain

$$
\begin{aligned}
\int_{-\frac{T}{2}}^{\frac{T}{2}} \phi_n^2(t)dt &= \int_{-\infty}^{\infty} \phi_n(t)\phi_n^D(t)dt \\
&= \frac{1}{2\pi}\int_{-\infty}^{\infty} \Phi_n(\omega)[\Phi_n^D(\omega)]^* d\omega \\
&= \frac{1}{2\pi\lambda_n}\int_{-\Omega}^{\Omega} S_{xx}(\omega)\left|\Phi_n^D(\omega)\right|^2 d\omega \\
&= \lambda_n,
\end{aligned}
\tag{40}
$$

and (26) follows.

To obtain the upper bound (33), we note from (31) and (32) that

$$\begin{aligned} J_{\min} &= \underline{J}_{\min} + \sum_{n=N}^{\infty} \phi_n^2(\tau + \tfrac{T}{2}) \frac{\sigma_e^2}{\lambda_n + \sigma_e^2} \\ &\leq \underline{J}_{\min} + \sum_{n=N}^{\infty} \phi_n^2(\tau + \tfrac{T}{2}) \\ &= \underline{J}_{\min} + \left[R_{xx}(0) - \sum_{n=0}^{N-1} \phi_n^2(\tau - \tfrac{T}{2}) \right] \\ &= R_{xx}(0) - \sum_{n=0}^{N-1} \phi_n^2(\tau + \tfrac{T}{2}) \frac{\lambda_n}{\lambda_n + \sigma_e^2}, \end{aligned} \tag{41}$$

where (30) was used, as in (31). From the bracketed expression in (41) it can be seen that, with (33), the difference $\overline{J}_{\min} - \underline{J}_{\min}$ will be small if $\sum_{n=0}^{N-1} \phi_n^2(\tau - \frac{T}{2})$ is close to $R_{xx}(0)$.

REFERENCES

[1] A. Duel-Hallen, S. Hu, and H. Hallen, "Long-range prediction of fading signals: Enabling adapting transmission for mobile radio channels," *IEEE Signal Processing Magazine*, vol. 17, no. 3, pp. 62–75, May 2000.

[2] G. E. Øien, H. Holm, and K. J. Hole, "Impact of channel prediction on adaptive coded modulation performance in Rayleigh fading," *IEEE Transactions on Vehicular Technology*, vol. 53, no. 3, pp. 758–769, May 2004.

[3] W. B. Davenport and W. L. Root, *An Introduction to the Theory of Random Signals and Noise*. New York: McGraw-Hill, 1958.

[4] R. J. Lyman and W. W. Edmonson, "Linear prediction of bandlimited processes with flat spectral densities," *IEEE Transactions on Signal Processing*, vol. 49, no. 7, pp. 1564–1569, July 2001.

[5] R. J. Lyman, "Optimal mean-square prediction of the mobile-radio fading envelope," *IEEE Transactions on Signal Processing*, vol. 51, no. 3, pp. 818–824, March 2003.

[6] T. Aulin, "A modified model for the fading signal at a mobile radio channel," *IEEE Transactions on Vehicular Technology*, vol. 28, no. 3, pp. 182–203, August 1979.

[7] R. J. Lyman and A. Sikora, "Prediction of fading envelopes with diffuse spectra," in *IEEE International Conference on Acoustics, Speech, and Signal Processing*, vol. 3, March 2005, pp. 753–756.

[8] G. L. Stuber, *Principles of Mobile Communication*. Boston: Kluwer, 1996.

[9] J. G. Proakis, *Digital Communications*, 4th ed. New York: McGraw-Hill, 2001.

[10] D. Slepian, H. J. Landau, and H. O. Pollak, "Prolate spheroidal wave functions, Fourier analysis and uncertainty–I & II," *Bell System Technical Journal*, vol. 40, no. 1, pp. 43–84, January 1961.

[11] R. H. Clarke, "A statistical theory of mobile radio reception," *Bell System Technical Journal*, vol. 47, no. 6, pp. 957–1000, July–August 1968.

[12] J. B. Andersen, J. Jensen, S. H. Jensen, and F. Frederiksen, "Prediction of future fading based on past measurements," in *Proceedings of the IEEE Vehicular Technology Conference*, September 1999.

[13] S. Qu and T. Yeap, "A three-dimensional scattering model for fading channels in land mobile environment," *IEEE Transactions on Vehicular Technology*, vol. 48, no. 3, pp. 765–781, May 1999.

[14] R. J. Lyman, W. W. Edmonson, M. Rao, and S. McCullough, "The predictability of continuous-time, bandlimited processes," *IEEE Transactions on Signal Processing*, vol. 48, no. 2, pp. 311–316, February 2000.

[15] A. Papoulis, "A note on the predictability of band-limited processes," *Proceedings of the IEEE*, vol. 73, no. 8, pp. 1332–1333, August 1985.

[16] W. H. Press, S. A. Teukolsky, W. T. Vetterling, and B. P. Flannery, *Numerical Recipes in C: The Art of Scientific Computing*, 2nd ed. New York: Cambridge University Press, 1992.

[17] B. R. Frieden, "Evaluation, design and extrapolation methods for optical signals, based on use of the prolate functions," in *Progress in Optics*. Amsterdam: North-Holland, 1971, vol. 9, pp. 311–407.

[18] A. Papoulis, *Signal Analysis*. New York: McGraw-Hill, 1977.

[19] W. C. Jakes, Ed., *Microwave Mobile Communications*. New York: Wiley, 1974.

[20] M. Abramowitz and I. A. Stegun, Eds., *Handbook of Mathematical Functions, with Formulas, Graphs, and Mathematical Tables*. New York: Dover Publications, Inc., 1965.

[21] K. E. Baddour and N. C. Beaulieu, "Autoregressive modeling for fading channel simulation," *IEEE Transactions on Wireless Communications*, vol. 4, no. 4, pp. 1650–1662, July 2005.

[22] A. J. Goldsmith and S. G. Chua, "Variable-rate variable-power MQAM for fading channels," *IEEE Transactions on Communications*, vol. 45, no. 10, pp. 1218–1230, October 1997.

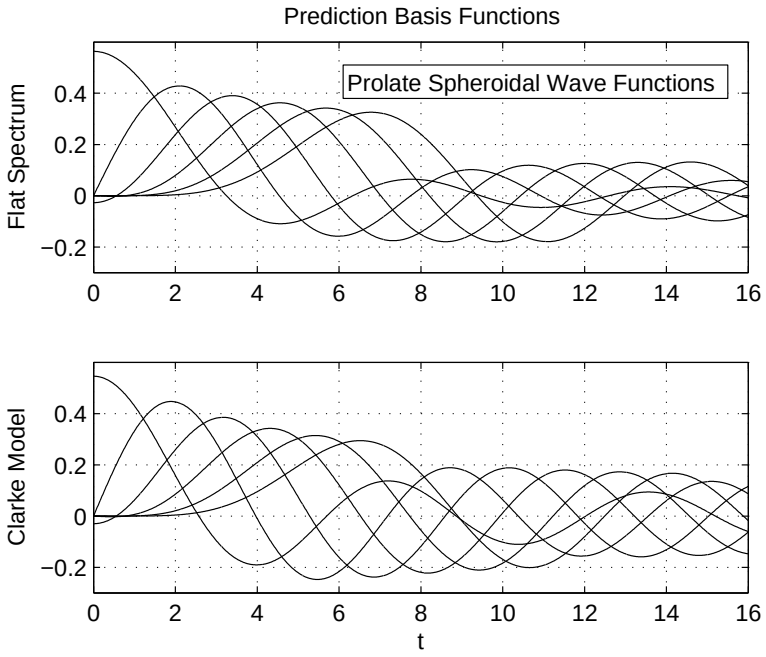

Fig. 1. Basis functions for prediction of fading envelopes with $\Omega = 1$ and $T = 2$.

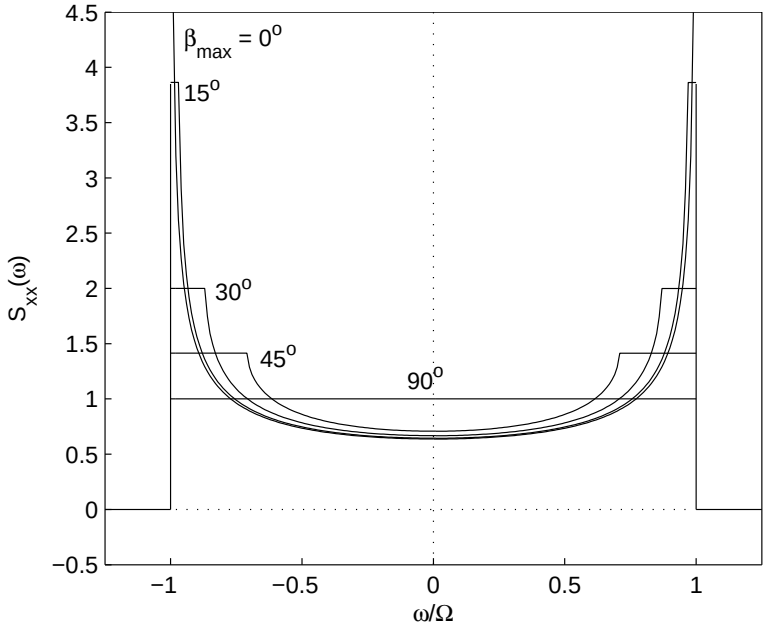

Fig. 2. Aulin-type fading spectra for various elevation angles $\beta_{\max}$.

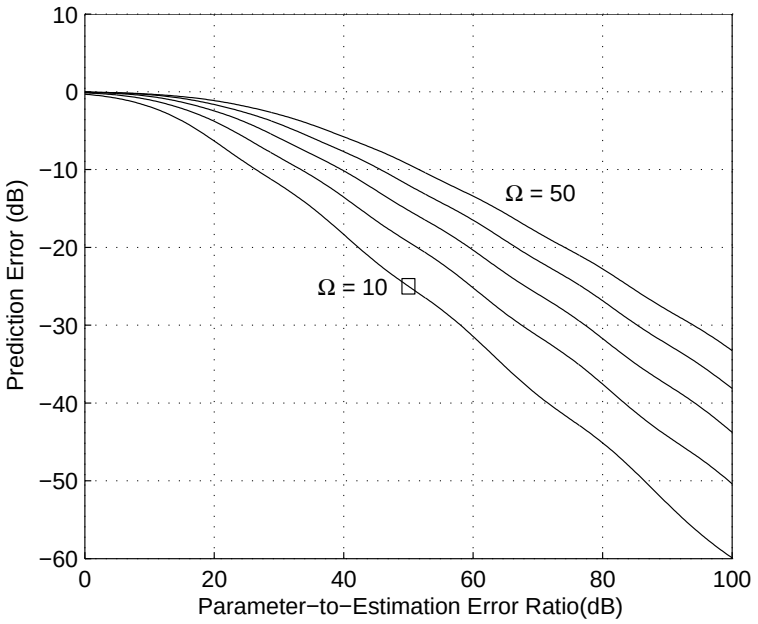

Fig. 3. Minimum mean squared prediction error of an Aulin-type fading envelope, $T = 0.2$ sec., $\tau = .04$ sec., and $\beta_{\max} = 30°$. The small box near the center of the graph represents the area covered by Figure 6.

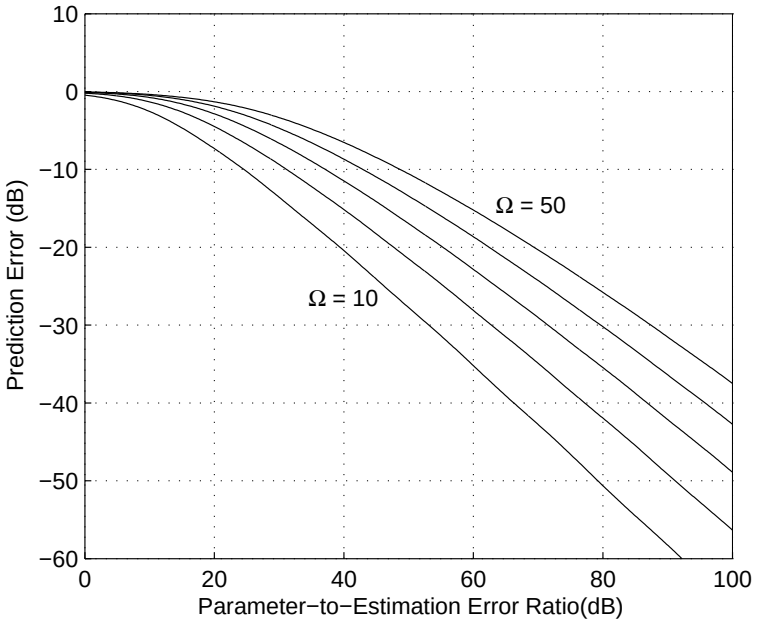

Fig. 4. In this figure, T has been increased to 0.8 sec. The graph reflects a small improvement in performance when the prediction is based on a longer interval of past values.

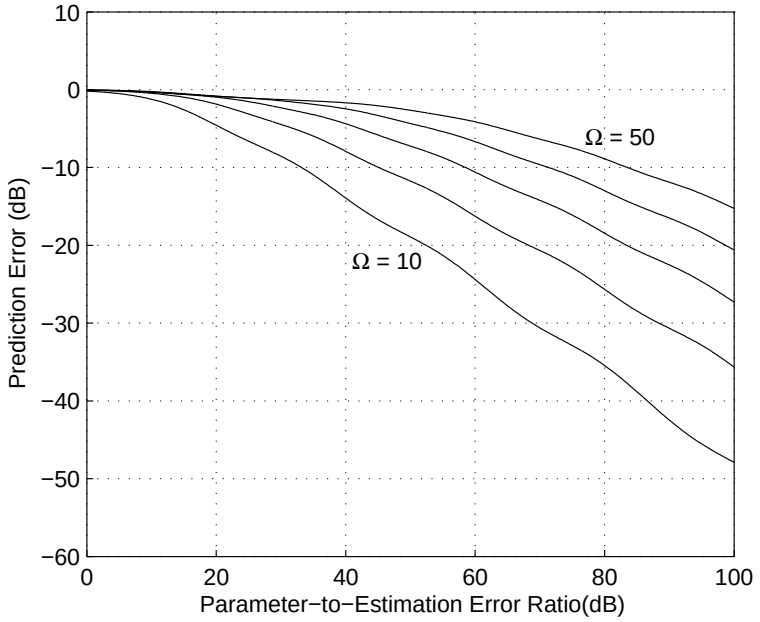

Fig. 5. In this case, $T = 0.2$ sec. again, and τ has been increased to .08 sec. The graph shows the performance degradation that occurs when we attempt to predict further into the future.

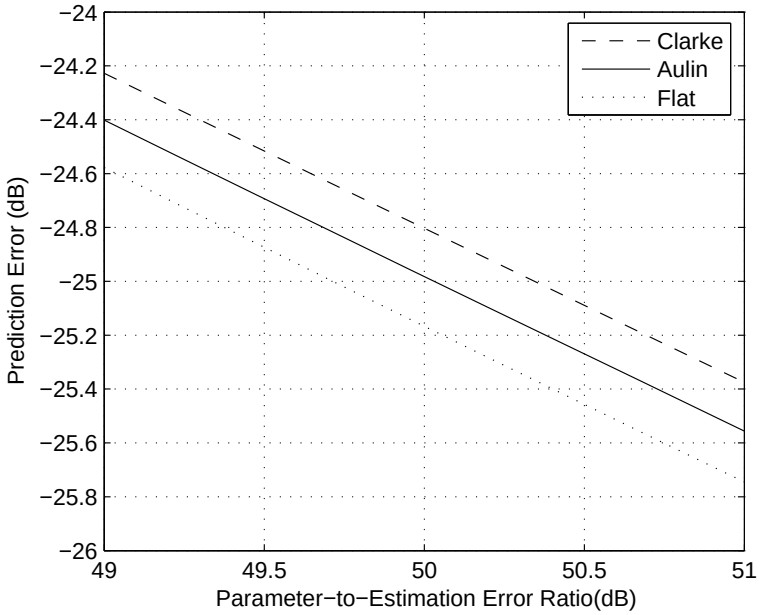

Fig. 6. This figure covers the area indicated by the small rectangle in Figure 3. The prediction parameters are $\Omega = 10$, $T = 0.2$ sec. and $\tau = .04$ sec. The three lines show prediction performance for fading envelopes with a Clarke spectrum, an Aulin spectrum with $\beta_{\max} = 30^{\circ}$, and a flat spectrum. Note that the performance variation is less than 0.4 dB.